nature astronomy

Article

https://doi.org/10.1038/s41550-023-02029-2

Detection of the cosmological time dilation of high-redshift quasars

Received: 6 January 2023

Accepted: 6 June 2023

Published online: 03 July 2023

Check for updates

Geraint F. Lewis [1] & Brendon J. Brewer [2]

A fundamental prediction of relativistic cosmologies is that, owing to the expansion of space, observations of the distant cosmos should be time dilated and appear to run slower than events in the local universe. While observations of cosmological supernovae unambiguously show the expected redshift-dependent time dilation, this has not been the case for other distant sources. Here we present the identification of cosmic time dilation in a sample of 190 quasars monitored for over two decades in multiple wavebands by assessing various hypotheses through Bayesian analysis. This detection counters previous claims that observed quasar variability lacked the expected redshift-dependent time dilation. Hence, as well as dismissing the claim that the apparent lack of the redshift dependence of quasar variability represents a substantial challenge to the standard cosmological model, this analysis further indicates that the properties of quasars are consistent with them being truly cosmologically distant sources.

A fundamental consequence of the relativistic picture of expanding space is cosmological time dilation, where events in the distant universe appear to run slowly compared with those in the local cosmos[1–3]. While this time dilation has been unambiguously detected in the light curves exhibited by cosmologically distant supernovae[4–8], the appearance of time dilation in other cosmic sources is less conclusive. For example, while examinations of the light curves of gamma-ray bursts have generally shown consistency with the expected cosmological signature, uncertainties in the detailed emission mechanism and expected light-curve characteristics mean that this detection has not been definitive (for example, refs. 9–13). Furthermore, the role of the more recently discovered fast radio bursts[14] as 'standard clocks' is similarly limited by knowledge of the physical processes driving the output[15].

Quasars have been known to be variable sources since their discovery in the 1960s[16], with emission arising from a relativistic accretion disk orbiting a supermassive black hole[17]. However, it has been claimed that the variability displayed by quasars over a broad range of redshifts does not show the expected cosmological time dilation[18–20]. This has led to the suggestion that quasar variability is not intrinsic, but is due to microlensing owing to the presence of cosmologically distributed black holes[21,22]. Others have stated that this points to more fundamental issues with our cosmological ideas (for example, refs. 23–25), with even the suggestion that quasars are not cosmologically distant and that their observed redshifts are due to mechanisms other than the expansion of space.

In 2012, a study of the variability characteristics of a sample of 13 quasars observed behind the Magellanic Clouds as part of the MACHO microlensing programme was suggestive of the expected $(1+z)$ time dilation dependence, where z is the quasar redshift[26]. However, with the small sample and relatively short monitoring period, this result is inconclusive. Recently, a new sample of the variability properties of quasars was presented as part of the Dark Energy Survey and comprises 190 quasars, covering the redshift range $z \approx 0.2$–4.0 (ref. 27). These are drawn from the sample of more than 100,000 spectroscopically identified quasars with absolute magnitude $M < -22$ in the 300 deg^2 Sloan Digital Sky Survey (SDSS) of Stripe 82. Published as part of the SDSS Data Release 7 quasar catalogue, the physical properties of these quasars are presented in ref. 28. This includes the bolometric luminosity, which was determined through spectral fitting and correction from composite spectral energy distributions[29]. These quasars were photometrically observed between 1998 and 2020, and so for more than two decades, through the combination of multiple epochs of exposures

[1]Sydney Institute for Astronomy, School of Physics, The University of Sydney, Sydney, New South Wales, Australia. [2]Department of Statistics, The University of Auckland, Auckland, New Zealand. e-mail: geraint.lewis@sydney.edu.au

https://doi.org/10.1038/s41550-023-02029-2

Table 1 | The marginal likelihoods for the various hypotheses considered in this paper

Hypothesis	n	$\log \mathcal{Z}$	$\mathcal{Z}/\mathcal{Z}_{max}$
H_0	0	−366.12	9.3×10^{-6}
H_1	1	−354.53	1
H_2	Free	−356.52	0.14
H_3	−1	−390.13	3.5×10^{-16}
H_4	2	−358.36	2.2×10^{-2}

As described in more detail in 'Methodology', these were calculated with the diffusive nested sampling approach DNest4[36]. Here, $\mathcal{Z}$ represents the Bayesian evidence, with the maximum value across the various hypotheses being $\mathcal{Z}_{max}$.

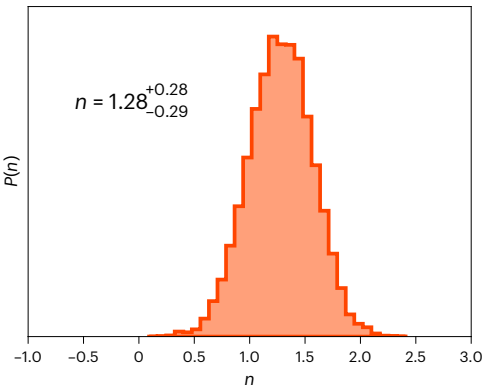

Fig. 1 | Posterior distribution of the redshift dependence for the time dilation. The posterior distribution of n, where the redshift dependence of the observed time dilation is given by $(1+z)^n$, for the Bayesian exploration of H_2, where this index is treated as a free parameter in the analysis. From this distribution, $n = 1.28^{+0.28}_{-0.29}$, where the best fit value is taken as the median (50th percentile), while the uncertainties represent the 16th and 84th percentiles. This distribution was determined through an exploration of the posterior probability space with DNest4[36].

from SDSS, Panoramic Survey Telescope and Rapid Response System 1 and the Dark Energy Survey, with additional follow-up monitoring with the Dark Energy Camera on the Blanco 4m.

The total dataset consists of roughly 200 photometric observations of each quasar in multiple bands, although the cadence of these observations is very uneven over the observing period. To account for this when calculating characteristic timescales of the quasar variabilities, ref. 27 adopted a Gaussian process regression (for example, ref. 30) to interpolate the photometric data and the associated uncertainties between the observations (details are given in Appendix A2 of their paper). Each quasar light curve in each band is represented as a damped random walk (DRW)[31,32]; this is found to be an accurate description of quasar variability with only a mild dependence on the physical properties of the quasars[33]. Practically, this defines the covariance matrix of the Gaussian process that describes the variability. With this, the Gaussian process regression software, celerite[34], is used to determine the characteristic DRW timescale, as well as the 16th and 84th percentiles of the distribution. Armed with these bolometric luminosities and variability timescales drawn from the DRW analysis, the goal of this paper is to search for the signature of cosmological time dilation of these distant sources.

Results

In the following analysis, we consider the redshift dependence of time dilation to be of the form $(1+z)^n$, where z is the redshift of the source. Clearly, for the expected cosmological dependence, $n = 1$, while $n = 0$ demonstrates no redshift dependence, representative of the claims from several previous studies of quasar samples (for example, ref. 20). To explore the various possibilities, several distinct hypotheses are explored. These are: H_0, n is fixed at zero, representing no redshift dependence on the observed quasar timescales; H_1, n is fixed at one, representing the expected redshift dependence of the cosmological time dilation; H_2, n is treated as a free parameter; H_3 and H_4, n is fixed at −1 and 2, respectively. The final two cases represent extreme cases where additional influences, such as quasar evolution, may substantially influence the observed time variability of quasars.

As outlined in 'Methodology', these differing hypotheses were compared through the calculation of the Bayesian evidence[35] for each situation under consideration, with the results of these calculations presented in Table 1; in assessing the ratio of Bayesian evidences, a factor of 10–100 is considered a strong favouring of one hypothesis over another, whereas greater than 100 is decisive[35]. One immediate conclusion is that the favoured hypothesis is H_1, the case where $n = 1$, which represents the expected redshift dependence of the cosmological time dilation. This is significantly favoured over the alternative H_0, with an evidence ratio greater than 10^5, which represents the situation where there is no redshift dependence on the observed timescales of cosmological variability. Furthermore, H_1 is significantly favoured over the two extreme cases, H_3 and H_4.

The posterior distribution of the redshift dependence for the time dilation, n, specifically H_2, where this is treated as a free parameter, is presented in Fig. 1. Reflecting the analysis presented previously, the value of n is clearly offset from zero, indicative of a redshift dependence of the observed timescale of variability over the quasar sample. This posterior distribution, which may be summarized using $n = 1.28^{+0.28}_{-0.29}$, is consistent with the expected cosmological dependence with $n = 1$, and the presented analysis significantly favours the presence of cosmological time dilation of the observed quasar variability.

Methodology

Probing the fundamental nature of our Universe often calls on standard rulers or candles to allow us to determine the influence of expansion on observable quantities. In hunting for cosmological time dilation, a standard clock with a measurable timescale is required. However, the challenge with objects such as quasars, and other cosmological sources such as gamma-ray bursts, is the complexity of the physical processes driving their variability. For quasars, where variability arises in the stochastic processes in the relativistic disk orbiting a supermassive black hole, the resultant luminosity fluctuations could potentially be dependent on a multitude of physical properties, including the mass of the central black hole, the degree of accretion and the wavelength of the observations.

To address this, the sample of quasars under consideration here was split into a number of subsamples of objects with similar intrinsic properties in terms of their bolometric luminosity and the rest wavelength of observations. The observations under consideration were taken in the (g, r, i) wavebands, and for the purpose of this study, the rest wavelength in each of the observed wavebands is defined to be

$$\lambda_g = \frac{4,720\,\text{Å}}{1+z}, \quad \lambda_r = \frac{6,415\text{Å}}{1+z}, \quad \lambda_i = \frac{7,835\text{Å}}{1+z} \tag{1}$$

where z is the redshift of the quasar under consideration and the numerical values are representative of the observed wavebands.

The quasar subsamples are presented graphically in Fig. 2, which presents the rest wavelengths of each quasar in the (g, r, i) bands versus their bolometric luminosity. Each quasar has been colour-coded with its variability timescale, τ_{DRW}, assessed by fitting each observed light curve in each band with a DRW (see ref. 27 for more detail). Underlying the quasar sample are the regions of 12 subsamples under consideration in the salmon pink colour. These were chosen to have a

https://doi.org/10.1038/s41550-023-02029-2

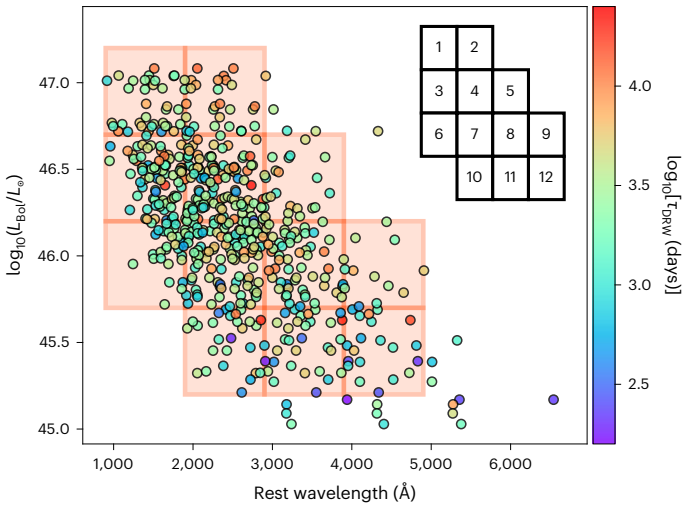

Fig. 2 | Quasar subsamples as a function of rest wavelength and bolometric luminosity. The entire quasar sample under consideration as a function of rest wavelength and bolometric luminosity, colour-coded with the DRW timescale, τ_{DRW}. The underlying rectangles in salmon pink represent the boundaries of the subsamples used in the analysis presented in this paper. Inset: the labelled numbers of the fields.

Table 2 | The properties of the survey quasar subsamples

Subsample	Δλ (Å)	$\Delta\log_{10}(L_{Bol}/L_{\odot})$	N_{qs}	Δz	$\Delta\log_{10}[\tau_{DRW}$ (days)]
1	900→1,900	46.7→47.2	37	1.60→4.15	2.68→4.03
2	1,900→2,900	46.7→47.2	27	0.81→3.00	2.83→4.11
3	900→1,900	46.2→46.7	74	1.55→3.98	2.61→4.23
4	1,900→2,900	46.2→46.7	111	1.11→3.01	2.49→4.42
5	2,900→3,900	46.2→46.7	22	1.11→1.70	3.03→3.93
6	900→1,900	45.7→46.2	30	1.48→2.80	2.70→3.71
7	1,900→2,900	45.7→46.2	101	0.68→2.80	2.55→3.92
8	2,900→3,900	45.7→46.2	58	0.60→1.69	2.63→4.03
9	3,900→4,900	45.7→46.2	11	0.60→1.00	2.66→3.84
10	1,900→2,900	45.2→46.7	27	0.63→1.45	2.30→4.30
11	2,900→3,900	45.2→46.7	31	0.47→1.45	2.27→4.30
12	3,900→4,900	45.2→46.7	20	0.47→0.98	2.33→4.20

The boundaries of the subsamples are given by Δλ, the rest wavelength, and $\Delta\log_{10}(L_{Bol}/L_{\odot})$, the bolometric luminosity. The remaining columns give the number of quasar light curves in each subsample, N_{qs}, as well as the redshift range of those quasars, Δz, and timescale for the observed variability as given by treating this as a DRW, $\Delta\log_{10}[\tau_{DRW}$(days)].

width in rest wavelength and bolometric luminosity of $\Delta\lambda = 1{,}000$ Å and $\Delta\log_{10}(L_{Bol}/L_{\odot}) = 0.5$. Note that the regions are continuous, with the top-left subsample spanning $\Delta\lambda = 900$ Å → 1,900 Å, and $\Delta\log_{10}(L_{Bol}/L_{\odot}) = 46.7 \rightarrow 47.2$; the details of the subsamples are given in Table 2. From Fig. 2, it is clear that these subsamples encompass the majority of quasars presented in this survey, and note that the combination of the three wavebands means that each subsample of quasars contains a broader distribution of redshifts than if the wavebands were considered individually. Hence this combination provides a redshift lever arm that constrains the presence of cosmological time dilation in each subsample. We also note that a by-eye examination of Fig. 2 is suggestive of a gradient in the variability timescale over the sample.

Given that in each subsample the quasars possess similar rest wavelengths and bolometric luminosities, we make the assumption that they also possess the same characteristic intrinsic timescales, and hence any difference in timescale for a particular quasar subsample is due to the influence of cosmic time dilation and will show the appropriate dependence upon redshift. Of course, the physics of quasar variability is likely to depend on a number of factors, and so this assumption is considering that these quasars will exhibit similar variability properties in the mean; we discuss this point again at the conclusion of this study.

For each quasar subsample (labelled with k), we model the observed variability timescales (that is, $\log_{10}[\tau_{DRW}$ (days)]) as

$$M_k = C_k + n\log_{10}(1+z) \quad (2)$$

where z is the redshift of the quasar and n is the power of the expected cosmological term, that is $(1+z)^n$. This model represents the variability with a different normalization term, C_k, for each wavelength–luminosity bin, but demands the same cosmological dependence in terms of redshift.

For the five distinct hypotheses considered, the normalization terms, C_k, were allowed to vary, and so for the cases where n is considered to be a fixed value, this corresponds to an exploration of a 12-dimensional posterior probability distribution. Physically, this situation reflects the situation where each wavelength–luminosity bin has a differing characteristic timescale, but a redshift dependence dependent upon the chosen value of n. For the remaining hypotheses, H_2, where C_k and n are treated as free parameters, this corresponds to a 13-dimensional posterior probability distribution to be explored.

To calculate the Bayesian evidence (also known as marginal likelihood) for each of these hypotheses, it is necessary to define a likelihood. It is important to note that the presented measurements and uncertainties of τ_{DRW} (in $\log_{10}$ space) are not symmetrical. Hence we represented the probability of each distribution of $\log_{10}[\tau_{DRW}$ (days)] as a skewed Gaussian, specifically scipy.stats.skewnorm in the numerical approach, which is written in Python (represented as $\mathcal{SN}$). The 16th, 50th and 84th percentiles of this skewed probability distribution function (PDF) were fitted to the given values via a straight-forward optimization. This resulted in uncertainties of these percentiles of typically less than 2–3%. Hence we can define the log of the likelihood as

$$\log\mathcal{L} = \sum_k \sum_{l=g,r,i} \sum_{m=1\ldots N_q} \mathcal{SN}\cdot\mathrm{logPDF}(\mathcal{M}_k, \theta_{l,m}(l, m \in k)) \quad (3)$$

where k sums over each of the subsample regions, l over the observed wavebands and m over the number of quasars, N_q, in the sample. Also, $\theta_{l,m}$ are the parameters for the skewed Gaussian representing the probability distribution for $\log_{10}[\tau_{DRW}$ (days)] for each of the quasars in each of the waveband, and $l, m \in k$ implies that the quasar should only be considered if its rest-frame properties place it in subsample k.

To explore the posterior probability distribution and calculate the Bayesian evidence (also known as marginal likelihood), we employed diffusive nested sampling (DNest4)[36], a variant of the nested sampling technique[37]. This allows for correct posterior sampling and marginal likelihood estimation even in the case where the constrained prior distributions are difficult to sample from or explore with Markov chain Monte Carlo. For simplicity, we use uniform priors over the normalization parameters, C_k, between 1 and 5, and for H_2 where n is treated as a free parameter, a uniform distribution over n is adopted between −1 and 3; the posterior distribution of n for this hypothesis is presented in Fig. 1. The normalizations, C_k, are well constrained and are reproduced for completeness in Fig. 3 for H_2.

Conclusions

This paper presents the detection of the cosmological dependence of the time dilation in a recent sample of almost 200 quasars. These were monitored in multiple wavebands over a two-decade period, allowing

https://doi.org/10.1038/s41550-023-02029-2

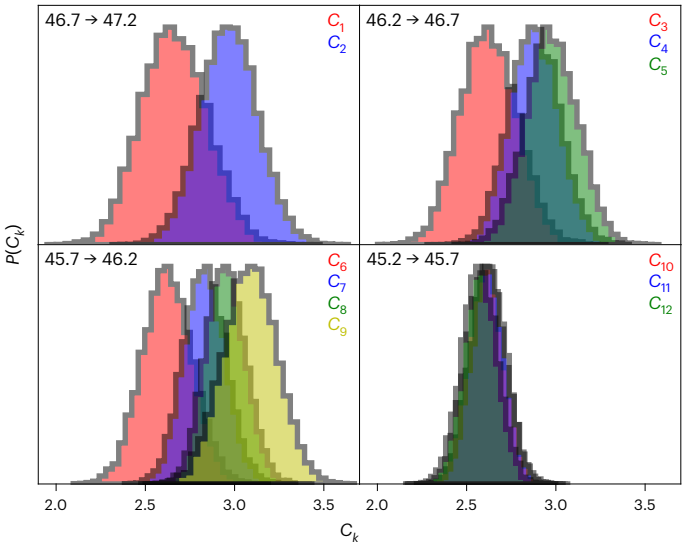

Fig. 3 | Posterior distributions for the normalization parameters. The posterior distributions for the normalization parameters, C_k, for H_2 where n is treated as a free parameter. The bolometric luminosity range for each of the normalization parameters is given in the top left of each panel (Table 2). As with Fig. 1, these were the result of the sampling of the posterior probability distribution with DNest4.

the determination of a characteristic timescale by treating the observed quasar variability as a DRW.

Through an assessment of the Bayesian evidence, it was found that the hypothesis considering the expected $(1+z)$ cosmological dependence provides a significantly better description of the data than the case where there is no dependence on redshift. In considering the redshift dependence of quasar variability to be of the form $(1+z)^n$, where n is treated as a free parameter, the posterior distribution is found to be $n = 1.28^{+0.28}_{-0.29}$, again consistent with the expected cosmological expansion of space. This detection of the cosmic expansion directly imprinted onto the variability of quasars further demonstrates that their observed properties are consistent with them being luminous and variable sources at cosmological distances, and counters previous claims that quasar variability is not intrinsic, but instead is due to external influences or non-standard physics. This has an immediate impact on various claims, such as the presence of a cosmologically dominant population of microlensing black holes (for example, refs. 18,22) or more esoteric ideas about the framework of the Universe[38], and is further evidence that we inhabit an expanding relativistic Universe.

We do note that our result of $n = 1.28^{+0.28}_{-0.29}$ could be consistent with an offset from the expected cosmological value of $n = 1$ and could potentially indicate the presence of additional factors such as an evolution of quasars over cosmic time in addition to the time dilation due to cosmic expansion. Of course, we could imagine that quasar evolution over cosmic time could be responsible for the observed redshift dependence of the DRW timescale, but as we are considering similar quasars in terms of the bolometric luminosity and observed rest wavelength, it would be a curious coincidence for this evolution to result in a $(1+z)$ dependence to spoof cosmic expansion. Furthermore, if quasar evolution were solely responsible for the observed DRW properties, then the resulting lack of the expected cosmic time dilation would present a severe challenge to our cosmological model. However, it is important to note that there are some potential correlations of the DRW timescales with the inferred intrinsic properties of the quasars (for example, ref. 33), although these are not strong, and more extensive photometric datasets in terms of the number of quasars and the duration of their photometric light curves will be required to cleanly separate the influence of cosmic expansion from quasar evolution.

In closing, we note that the lack of detection of the time dilation of quasar variability in previous studies is potentially due to the relatively small sample size in terms of the number of quasars under consideration[26], or the cadence of data sampling and characterization of the quasar variability[19,20]. Built on the observations of ref. 27, this present study has demonstrated that we are now in an epoch where we have observations of a sufficiently large number of quasars spanning a broad range in redshifts, and observed over extended periods and with a cadence that overcomes their stochastic nature and results in an accurate characterization of their variability, yielding a robust determination of the imprint of cosmological expansion on their light curves. Furthermore, with upcoming programmes such as the Vera Rubin Observatory Legacy Survey of Space and Time, the number of quasars observed at high temporal cadence will rapidly increase and the measurement of cosmological time dilation, and potentially the influence of quasar evolution, will become readily observable (for example, ref. 32).

Data availability

The source data for this project are available at https://zenodo.org/record/5842449#.YipOg-jMJPY, with the details of the available FITS tables presented in ref. 27. Note that a revised version of this catalogue was recently released due to an error in some rest-frame quantities. This revision does not impact any of the research presented in this paper. The software for this project is available at https://github.com/eggplantbren/QuasarTimeDilation.

Code availability

This project made use of several publicly available software packages, especially DNest4[36] to undertake the exploration of the posterior probability space and calculate the Bayesian evidence by integrating across this space. Further software packages employed include matplotlib[39], numpy[40] and scipy[41]. Initial explorations of the posterior probability space were undertaken with emcee with corner plots prepared with corner[42]. The software employed as part of this project will be made available on reasonable request to the corresponding author.

References

1. Lemaître, G. et al. Un Univers homogène de masse constante et de rayon croissant rendant compte de la vitesse radiale des nébuleuses extra-galactiques. *Ann. Soc. Sci. Bruxelles* **47**, 49–59 (1927).
2. Lemaître, G. et al. A homogeneous universe of constant mass and increasing radius accounting for the radial velocity of extra-galactic nebulae. *Mon. Not. R. Astron. Soc.* **91**, 483–490 (1931).
3. Wilson, O. C. Possible applications of supernovae to the study of the nebular red shifts. *Astrophys. J.* **90**, 634 (1939).
4. Leibundgut, B. et al. Time dilation in the light curve of the distant type IA supernova SN 1995K. *Astrophys. J. Lett.* **466**, L21 (1996).
5. Riess, A. G. et al. Time dilation from spectral feature age measurements of type IA supernovae. *Astron. J.* **114**, 722–729 (1997).
6. Goldhaber, G. et al. Timescale stretch parameterization of type Ia supernova B-band light curves. *Astrophys. J.* **558**, 359–368 (2001).
7. Foley, R. J. et al. A definitive measurement of time dilation in the spectral evolution of the moderate-redshift type Ia supernova 1997ex. *Astrophys. J. Lett.* **626**, L11–L14 (2005).
8. Blondin, S. et al. Time dilation in type Ia supernova spectra at high redshift. *Astrophys. J.* **682**, 724–736 (2008).
9. Norris, J. P. et al. Detection of signature consistent with cosmological time dilation in gamma-ray bursts. *Astrophys. J.* **424**, 540 (1994).

10. Kocevski, D. & Petrosian, V. On the lack of time dilation signatures in gamma-ray burst light curves. *Astrophys. J.* **765**, 116 (2013).
11. Zhang, F.-W., Fan, Y.-Z., Shao, L. & Wei, D.-M. Cosmological time dilation in durations of swift long gamma-ray bursts. *Astrophys. J. Lett.* **778**, L11 (2013).
12. Littlejohns, O. M. & Butler, N. R. Investigating signatures of cosmological time dilation in duration measures of prompt gamma-ray burst light curves. *Mon. Not. R. Astron. Soc.* **444**, 3948–3960 (2014).
13. Singh, A. & Desai, S. Search for cosmological time dilation from gamma-ray bursts—a 2021 status update. *J. Cosmol. Astropart. Phys.* **2022**, 010 (2022).
14. Petroff, E., Hessels, J. W. T. & Lorimer, D. R. Fast radio bursts at the dawn of the 2020s. *Astron. Astrophy. Rev.* **30**, 2 (2022).
15. Zhang, B. The physics of fast radio bursts. Preprint at *arXiv* https://doi.org/10.48550/arXiv.2212.03972 (2022).
16. Schmidt, M. 3C 273: a star-like object with large red-shift. *Nature* **197**, 1040 (1963).
17. Salpeter, E. E. Accretion of interstellar matter by massive objects. *Astrophys. J.* **140**, 796–800 (1964).
18. Hawkins, M. R. S. Gravitational microlensing, quasar variability and missing matter. *Nature* **366**, 242–245 (1993).
19. Hawkins, M. R. S. Time dilation and quasar variability. *Astrophys. J. Lett.* **553**, L97–L100 (2001).
20. Hawkins, M. R. S. On time dilation in quasar light curves. *Mon. Not. R. Astron. Soc.* **405**, 1940–1946 (2010).
21. Hawkins, M. R. S. & Taylor, A. N. Quasar variability and gravitational microlensing. *Astrophys. J. Lett.* **482**, L5–L8 (1997).
22. Hawkins, M. R. S. New evidence for a cosmological distribution of stellar mass primordial black holes. *Mon. Not. R. Astron. Soc.* **512**, 5706–5714 (2022).
23. Chashchina, O. I. & Silagadze, Z. K. Expanding space, quasars and St. Augustine's fireworks. *Universe* **1**, 307–356 (2015).
24. López-Corredoira, M. Tests and problems of the standard model in cosmology. *Found. Phys.* **47**, 711–768 (2017).
25. Crawford, D. F. A problem with the analysis of type Ia supernovae. *Open Astron.* **26**, 111–119 (2017).
26. Dai, D.-C., Starkman, G. D., Stojkovic, B., Stojkovic, D. & Weltman, A. Using quasars as standard clocks for measuring cosmological redshift. *Phys. Rev. Lett.* **108**, 231302 (2012).
27. Stone, Z. et al. Optical variability of quasars with 20-yr photometric light curves. *Mon. Not. R. Astron. Soc.* **514**, 164–184 (2022).
28. Shen, Y. et al. A catalog of quasar properties from Sloan Digital Sky Survey Data Release 7. *Astrophys. J. Suppl. Ser.* **194**, 45 (2011).
29. Richards, G. T. et al. Spectral energy distributions and multiwavelength selection of type 1 quasars. *Astrophys. J. Suppl. Ser.* **166**, 470 (2006).
30. Aigrain, S. & Foreman-Mackey, D. Gaussian process regression for astronomical time-series. Preprint at *arXiv* https://doi.org/10.48550/arXiv.2209.08940 (2022).
31. Kelly, B. C., Bechtold, J. & Siemiginowska, A. Are the variations in quasar optical flux driven by thermal fluctuations? *Astrophys. J.* **698**, 895–910 (2009).
32. Sheng, X., Ross, N. & Nicholl, M. Legacy Survey of Space and Time cadence strategy evaluations for active galactic nucleus time-series data in Wide-Fast-Deep field. *Mon. Not. R. Astron. Soc.* **512**, 5580–5600 (2022).
33. Suberlak, K. L., Ivezić, Ž. & MacLeod, C. Improving damped random walk parameters for SDSS Stripe 82 quasars with Pan-STARRS1. *Astrophys. J.* **907**, 96 (2021).
34. Foreman-Mackey, D., Agol, E., Angus, R. & Ambikasaran, S. Fast and scalable gaussian process modeling with applications to astronomical time series. *Astron. J.* **154**, 220 (2017).
35. Kass, R. E. & Raftery, A. E. Bayes factors. *J. Am. Stat. Assoc.* **90**, 773–795 (1995).
36. Brewer, B. J. & Foreman-Mackey, D. DNest4: diffusive nested sampling in C++ and Python. *J. Stat. Softw.* **86**, 1–33 (2018).
37. Skilling, J. Nested sampling. *AIP Conf. Proc.* **735**, 395–405 (2004).
38. Sanejouand, Y.-H. A framework for the next generation of stationary cosmological models. *Int. J. Mod. Phys. D* **31**, 2250084 (2022).
39. Hunter, J. D. Matplotlib: a 2D graphics environment. *Comput. Sci. Eng.* **9**, 90–95 (2007).
40. Harris, C. R. et al. Array programming with NumPy. *Nature* **585**, 357–362 (2020).
41. Virtanen, P. et al. SciPy 1.0: fundamental algorithms for scientific computing in Python. *Nat. Methods* **17**, 261–272 (2020).
42. Foreman-Mackey, D. corner.py: scatterplot matrices in Python. *J. Open Source Softw.* **1**, 24 (2016).

Acknowledgements

We thank Z. Stone et al.[27] for making their data and the results of their analysis publicly available. We also thank S. Croom for his input and advice on quasar variability surveys. We further thank the teams responsible for creating and maintaining the various software packages, detailed below, that this study has employed. G.F.L. thanks the hospitality of the Lowell Observatory where the last stages of this work were completed during a period of isolation due to the contraction of COVID-19.

Author contributions

The project was conceived by G.F.L., including an initial exploration of the data, the definition of the models and hypotheses considered, the likelihood function and sampling of the posterior space. B.J.B. undertook detailed sampling and calculating the Bayesian evidence using DNest4. Both authors discussed the results of the exploration in detail, determined the resulting conclusion and were responsible for the writing of the paper.

Competing interests

The authors declare no competing interests.

Additional information

Correspondence and requests for materials should be addressed to Geraint F. Lewis.

Peer review information *Nature Astronomy* thanks Deborah Dultzin and the other, anonymous, reviewer(s) for their contribution to the peer review of this work.